1.E.3: 2.N *Nuclear Physics* **A261** (1976) 498–510; © *North-Holland Publishing Co., Amsterdam*

REORIENTATION EFFECT MEASUREMENTS OF ^{122}Te AND ^{130}Te

A. BOCKISCH and A. M. KLEINFELD
1. Physikalisches Institut der Universität zu Köln, 5 Köln 41, W. Germany

Received 29 December 1975

Abstract: Coulomb excitation probabilities of the first 2^+ states of ^{122}Te and ^{130}Te have been determined. The measurement was performed by resolving the inelastically and elastically scattered ^{4}He and ^{16}O projectiles using eight surface barrier detectors between 44° and 173°. Quadrupole moments Q_{2+} as well as $B(\mathrm{E2}, 0^+ \rightarrow 2^+)$ values were deduced. The Q_{2+} found for the positive sign of the 2_2^+ interference term are $-0.46 \pm 0.05\ e \cdot \mathrm{b}$ and $-0.15 \pm 0.10\ e \cdot \mathrm{b}$ for ^{122}Te and ^{130}Te respectively.

E NUCLEAR REACTIONS ^{122,130}Te(α, α'), $E = 10$–11 MeV, ^{122,130}Te(^{16}O, ^{16}O'), $E = 30$–54 MeV; measured $\sigma(E_{16_O}, E_{16_{O'}})$, $\sigma(E_\alpha, E_{\alpha'})$. ^{122,130}Te deduced Q_{2+}, $B(\mathrm{E2}, 0^+ \rightarrow 2^+)$. Enriched targets.

1. Introduction

Interest in the doubly even vibrational like nuclei [1]) has spurred a large number of measurements of the static electric quadrupole moments (Q_{2+}) of their first 2^+ states. In particular, the Te isotopes have been the subject of several investigations [refs. [2–7])]. The present study completes a series of measurements of the Q_{2+} and $B(\mathrm{E2}, 0_1^+ \rightarrow 2_1^+)$ values of the doubly even isotopes of tellurium between ^{122}Te and ^{130}Te. Part of this study, including the isotopes ^{124}Te, ^{126}Te and ^{128}Te, has previously been reported [6]). Moreover in the present work an investigation of the scattering angle as well as the projectile mass dependence of the effect has been carried out for ^{122}Te. We find that the result of the measurements of all the tellurium isotopes are in excellent agreement with one another. The Q_{2+} is found to increase from -0.47 $e \cdot \mathrm{b}$ for ^{122}Te to $-0.12\ e \cdot \mathrm{b}$ for ^{130}Te. As a consequence a set of accurate Q_{2+} and $B(\mathrm{E2}, 0_1^+ \rightarrow 2_1^+)$ values now exists for which a meaningful comparison with nuclear models may be made.

2. Experimental details

The measurements were performed using the reorientation effect [8]) of Coulomb excitation. The experimental method was similar to that used in refs. [6, 9]) where more details of the technique may be found. In addition to the projectile mass dependence of the effect used in refs. [6, 9]), a measurement of the effect as a function of projectile scattering angle was performed in the present study, which afforded us an additional check of the method.

Beams of 10–11 MeV ^{4}He and 30–54 MeV ^{16}O were obtained from the Köln FN tandem accelerator. Intensities were kept below 30 and 10 nA for ^{4}He and ^{16}O respectively to minimize target degradation. Targets were composed of thin layers (about 30 μg/cm^2 for ^{4}He and 10 μg/cm^2 for ^{16}O) of enriched isotopes, vacuum evaporated onto 10–20 μg/cm^2 carbon backings. The suppliers assay of the isotopic composition of the target material is given in table 1. Several remarks concerning the target composition are appropriate. As explained below the measurement method used in the present study (most important in this regard are the 173° spectra) enabled us to perform an independent analysis of most of the isotopic composition of the ^{122}Te material. It was found that while the assays of the first two samples were accurate, some errors were discovered in the assay of sample 3. This amounted to differences of about 15 % for ^{130}Te, 15 % for ^{128}Te, 6 % for ^{125}Te and 9 % for ^{124}Te, between the suppliers assay and our own analysis. However in spite of this discrepancy all three samples yielded consistent results where overlap in the data occurred. This lends confidence to the handling of the impurity isotope subtraction discussed below.

TABLE 1

Isotopic concentration of the target material (%)

	Target	Impurity (%)							
		120	122	123	124	125	126	128	130
1	122	<0.04	91.40	0.65	0.95	0.95	1.90	2.07	1.80
2	122	<0.03	95.07	0.41	0.64	0.62	1.07	1.13	1.06
3	122	<0.04	88.4	1.40	1.70	1.30	2.30	2.60	2.40
4	130	<0.02	0.04	0.02	0.02	0.03	0.10	0.30	99.49

Samples 1, 2 and 4 were obtained from Oak Ridge and the suppliers' assay is given. Sample 3 was obtained from Iso-commerz and, as explained in the text, the assay was in part determined from the analysis of the backscattered ^{16}O spectra.

Ions scattered from the targets were detected in eight surface barrier detectors of 100 μm thickness, at lab angles between 44° and 173°. Considerable effort was made to accurately determine scattering angles. This is especially important at the forward angles, where e.g. a change in the scattering angle by 1° at 45°, produces a 7 % change in the excitation probability. For this reason the scattering chamber for which detectors could be placed only at fixed angles (every 15°) was particularly advantageous. Several independent measurements of the scattering angles were performed [10]) all of which yielded consistent results (given in table 2). The scattering angle errors were estimated to be $\pm 0.2°$.

The detector system resolution was sufficient to resolve elastically scattered ions and those inelastically scattered from the first 2_1^+ states at 0.564 and 0.846 MeV for ^{122}Te and ^{130}Te respectively. Typical spectra are shown in figs. 1–3. The resolution (FWHM) obtained was about 30–40 keV for ^{4}He and 100–150 keV for ^{16}O. More

TABLE 2

Experimental excitation probabilities (R_{exp}) of the 2_1^+ state used in the analysis

Projectile	E_{eff} (MeV)	Scatt. angle	$10^3\ R_{exp}(2_1^+)$	Error %
		^{122}Te		
^{4}He	10.0	173.4	7.24	1.3
	10.0	173.4	7.16	1.2
	10.5	173.4	8.96	2.4
	10.5	173.4	8.99	1.5
	10.5	173.4	9.08	1.2
	10.5	173.4	8.85	1.3
	10.5	173.4	8.78	1.3
^{16}O	54.0	59.2	42.26	1.8
	54.0	74.2	73.32	1.5
	38.0	89.3	28.51	5.8
	40.0	89.3	29.07	10.3
	40.0	89.3	34.29	5.1
	45.0	89.3	61.61	10.7
	45.0	89.3	57.00	6.8
	50.0	89.3	76.00	2.8
	54.0	89.3	105.1	1.5
	38.0	103.7	36.60	13.5
	43.0	103.7	53.22	8.8
	46.0	103.7	79.52	5.9
	50.0	103.7	103.6	3.4
	35.0	120.2	27.72	10.8
	38.0	120.2	42.12	6.5
	40.0	120.2	56.74	7.4
	40.0	120.2	54.88	5.7
	42.0	120.2	62.98	12.5
	43.0	120.2	64.58	7.2
	45.0	120.2	96.28	7.3
	45.0	120.2	91.09	9.6
	46.0	120.2	94.71	3.5
	47.0	120.2	108.1	4.6
	50.0	120.2	128.6	10.0
	50.0	120.2	134.2	2.9
	30.0	135.4	13.60	14.6
	38.0	135.4	57.65	7.3
	38.0	135.4	51.19	7.6
	40.0	135.4	55.62	20.3
	40.0	135.4	58.84	7.8
	40.0	59.97	59.97	5.9
	43.0	135.4	86.30	5.0
	45.0	135.4	103.5	8.5
	45.0	135.4	97.47	9.5
	45.0	135.4	102.4	8.2
	46.0	135.4	110.7	3.3
	47.0	135.4	115.9	5.4
	50.0	135.4	142.9	2.9
	50.0	135.4	138.7	10.9
	35.0	173.4	32.58	6.2

TABLE 2 (continued)

Projectile	E_{eff} (MeV)	Scatt. angle	$10^3 R_{exp}(2_1^+)$	Error %
		^{122}Te		
	38.0	173.4	49.69	4.4
	38.0	173.4	56.07	2.2
	40.0	173.4	71.78	5.5
	40.0	173.4	71.70	1.2
	42.0	173.4	87.41	5.6
	43.0	173.4	95.92	1.5
	45.0	173.4	112.1	1.8
	46.0	173.4	125.8	0.93
	47.0	173.4	135.3	1.4
	50.0	173.4	158.4	4.6*
	50.0	173.4	159.1	1.7*
	52.5	173.4	177.8	2.7*
		^{130}Te		
^{4}He	10.5	173.4	2.17	2.7
	10.5	173.4	2.28	2.2
	10.5	173.4	2.20	3.1
^{16}O	42.0	89.3	13.00	8.8
	42.0	89.3	13.47	3.3
	44.0	89.3	15.75	4.9
	44.0	89.3	16.84	4.3
	44.0	89.3	16.09	4.8
	44.0	89.3	17.04	4.6
	47.0	89.3	22.05	9.5
	50.0	89.3	30.30	5.2
	52.5	89.3	34.48	5.0
	42.0	120.2	19.32	7.8
	42.0	120.2	20.53	10.4
	44.0	120.2	23.92	6.6
	49.0	120.2	40.62	4.7
	51.0	120.2	52.12	4.4
	42.0	135.4	23.97	15.5
	44.0	135.4	27.96	6.4
	44.0	135.4	27.79	4.8
	49.0	135.4	46.24	4.6
	51.0	135.4	56.60	5.4*
	42.0	173.4	24.26	3.1
	42.0	173.4	24.32	1.5
	44.0	173.4	30.86	2.2
	44.0	173.4	31.10	2.3
	44.0	173.4	30.83	1.9
	47.0	173.4	44.92	4.0
	49.0	173.4	52.91	1.6*
	50.0	173.4	56.33	2.5*
	51.0	173.4	61.62	1.8*
	52.5	173.4	64.05	2.3*

Values have been corrected for various effects mentioned in the text. Those with an asterisk have not been used for extracting the B(E2) and Q_{2+} values.

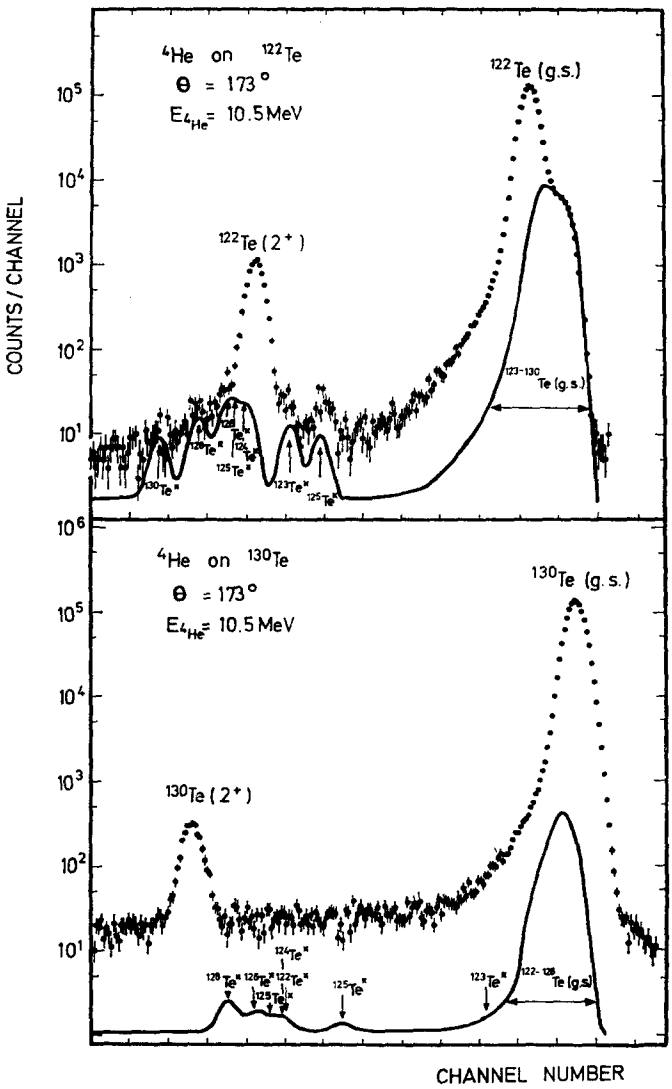

Fig. 1. Spectra of ^{4}He on ^{122}Te and ^{130}Te respectively at $\theta = 173°$. The solid line represents the contribution due to elastic (Te(g.s.)) and inelastic (Te*) scattering from the tellurium impurities.

important for an accurate determination of the excitation probabilities are the ratios of the inelastic peak heights to the background. Values of about 100:1 and 20:1 for the ^{4}He spectra of ^{122}Te and ^{130}Te respectively were typical. While values for the ^{16}O spectra ranged between 5:1 and better than 30:1 depending upon scattering angle, energy and isotope.

The major experimental problem was to determine the excitation probability (R) of the 2_1^+ states, as a function of projectile mass and scattering angle, with an accuracy

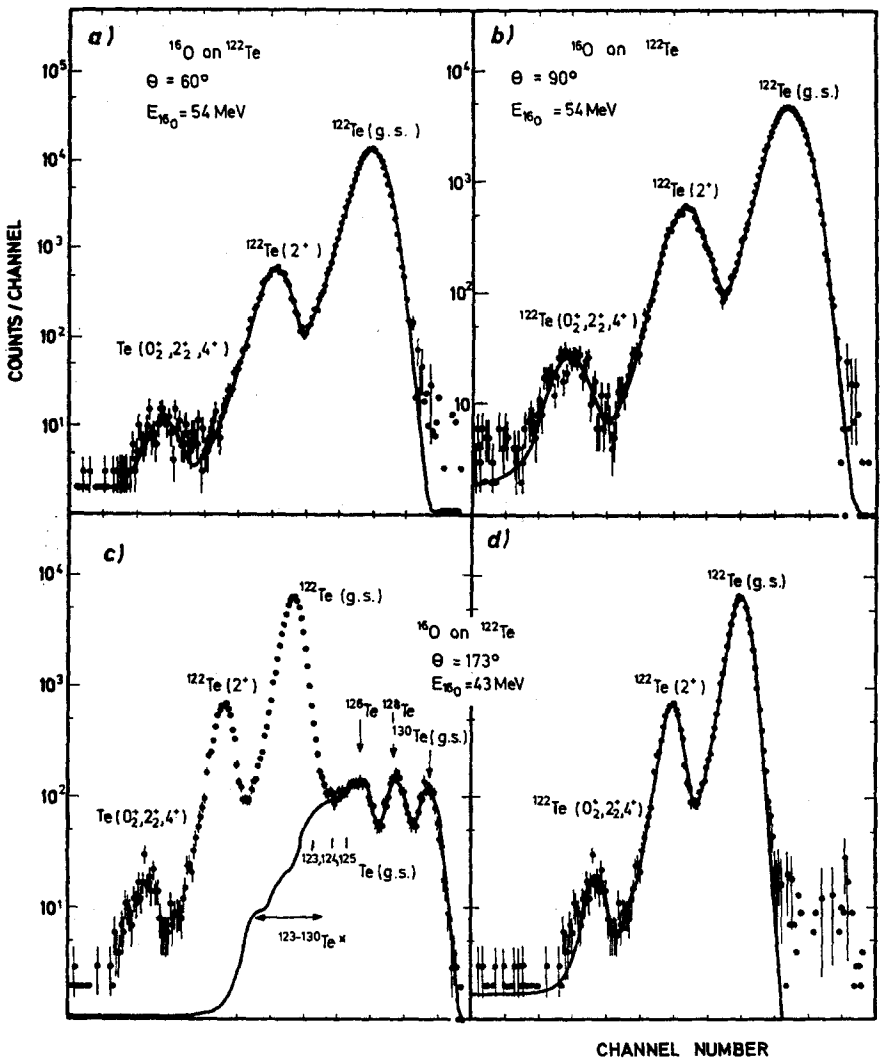

Fig. 2. Spectra of ^{16}O on ^{122}Te at 60°, 90° and 173°. In part (c) a spectrum before impurity subtraction is shown. The solid line in (c) has been calculated from the known impurity contributions. The solid lines shown in (a), (b) and (d) were obtained from line-shape fits to the spectra after subtraction of the impurity contribution.

of about 1 %. This accuracy corresponds to an error of about $\pm 0.1\ e \cdot b$ in Q_{2^+}. The 2_1^+ intensity was evaluated using the line shape programs of ref. [6]) where the fits, as shown in figs. 1–3, were used to obtain the background under the 2_1^+ peak and to assure that the peak shape was consistent with a single peak. The results of this analysis together with the corresponding uncertainties, bombarding energies and laboratory scattering angles are shown in table 2.

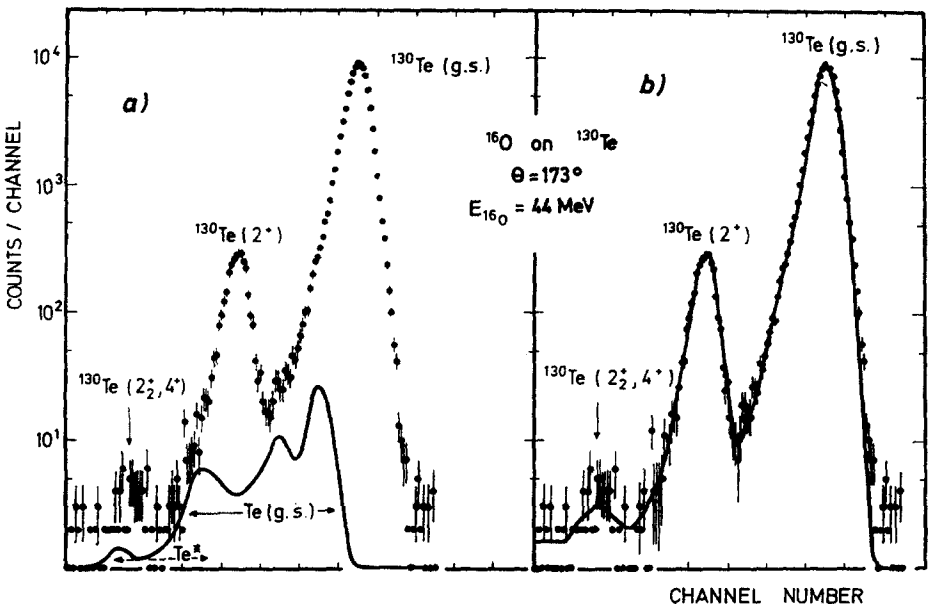

Fig. 3. Spectrum of ^{16}O on ^{130}Te at $\theta = 173°$, showing (a) the spectrum before impurity subtraction and (b) after. The solid lines represent the calculated impurity contributions and the line-shape fit to (a) and (b) respectively.

The high degree of accuracy required for the excitation of the 2_1^+ intensities necessitates careful consideration of the possibility of contamination. The solid curves in figs. 2c and 3c have been generated using the elastic line shape, the supplier's assay (samples 1 and 2 for ^{122}Te) for the isotopic composition of the target material and the known [6,11]) B(E2) values for inelastic contributions. As is seen in fig. 2c the agreement between the measured intensities and the supplier's assay, with the exception of sample 3 as discussed above, is excellent. For sample 3 a fit to the resolved impurity isotopes (124–130) was performed. The isotopic abundances were obtained from the fit with an accuracy of about 0.1 % and are given in col. 3 of table 1. Although ^{123}Te is unresolved no difficulty ensues since its natural abundance is only 0.89 % and it does not contribute to the inelastic (2_1^+ of ^{122}Te) intensity. The only error in subtracting out these contributions, in the case of ^{122}Te, is therefore due to the uncertainties in the B(E2) values. The total uncertainty in R from this source is less than 0.2 %. Since the contaminent isotopes are not resolved the situation is less clear in the case of ^{130}Te. However the only material used was obtained from Oak Ridge and had a nominal enrichment for ^{130}Te of 99.49 %. We therefore concluded that for ^{130}Te the error in R due to uncertainties in the target composition and B(E2) values was about 0.5 %. Other contributions due to e.g. elastic scattering from lighter mass impurities can be estimated from the combination of ^{4}He and ^{16}O spectra taken at various angles and energies. Uncertainties in R from such effects

were less than 0.05–0.5 % for ^{122}Te and less than 0.5 % for ^{130}Te. From ^{16}O and ^{4}He spectra of the carbon backings alone we determined that contributions to the elastic and inelastic Te intensities from this source were not present.

Essential for validity of the analysis is that contributions to the 2_1^+ intensities from sources other than pure Coulomb excitation (i.e. nuclear reactions) are negligible. Hence the data used in the analysis must correspond to projectile energies com-

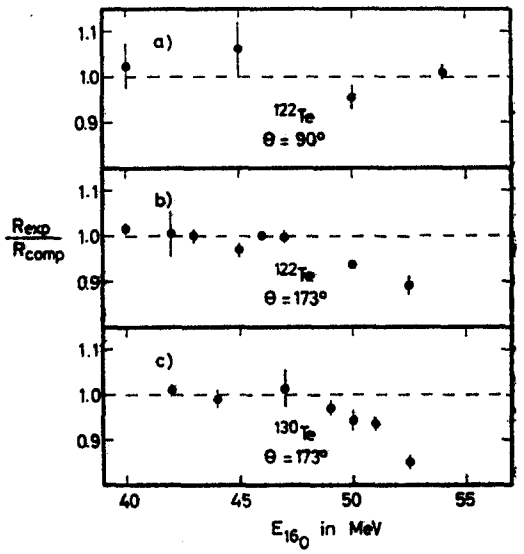

Fig. 4. Normalized excitation function for ^{122}Te and ^{130}Te at 173° and ^{122}Te at 90°.

$$\begin{pmatrix} 0 & \pm M_{12} & 0 & .10 & 0 & .07 \\ \pm M_{12} & M_{22} & 1.33 & .93 & .34 & \pm .26 \\ 0 & 1.33 & 0 & 0 & 0 & 0 \\ .10 & .93 & 0 & 0 & 0 & 0 \\ 0 & .34 & 0 & 0 & 0 & 0 \\ .07 & \pm .26 & 0 & 0 & 0 & 0 \end{pmatrix} \qquad \begin{pmatrix} 0 & \pm M_{12} & 0 & .07 \\ \pm M_{12} & M_{22} & .86 & .37 \\ 0 & .86 & 0 & 0 \\ .07 & .37 & 0 & 0 \end{pmatrix}$$

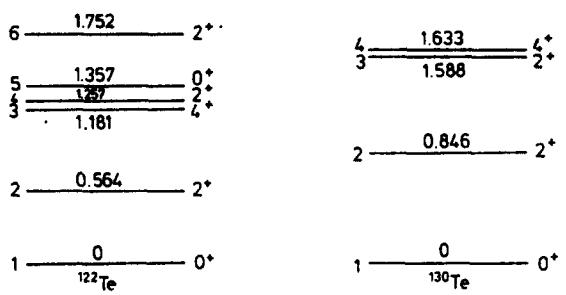

Fig. 5. Energy levels and E2 matrix elements used in the analysis of ^{122}Te and ^{130}Te respectively. The 2_3^+ assignment for the level at 1.752 MeV was taken from ref. [5]).

patible with the "safe energy". For this purpose excitation functions of the 2_1^+ states for ^{16}O on ^{122}Te and ^{130}Te were measured. From the results of these measurements, which are presented in fig. 4 and those of ref. [12]), a safe energy of 47 MeV for 173° and greater than 54 MeV for angles less than 90° for both isotopes were adopted. In a previous investigation [6]) it was shown that for ^4He energies up to and including 10.5 MeV the deviations from pure Coulomb excitation were less than 1 %.

3. Analysis

To obtain the Q_{2+} and $B(E2, 0_1^+ \rightarrow 2_1^+)$ values, the analysis of the data followed the procedure discussed in ref. [9]). The E2 matrix elements and energy levels used in the de Boer-Winther [13]) program to generate the calculated R-values (R_{comp}) are shown in fig. 5. Matrix elements of the 2_2^+ and 4_1^+ states of ^{130}Te were obtained [14]) by comparing the sum (energy separation is 45 keV) of the excitation probabilities with the corresponding R_{comp} values. These values are in good agreement with those of ref. [3]). In the case of ^{130}Te a more precise determination of these matrix elements is unnecessary since Q_{2+} is only weakly dependent upon these values, as witnessed by the small change in Q_{2+} (about 0.08 $e \cdot b$) for a change in the sign of the interference term. Indeed the insensitivity to this sign made its determination in the case of ^{130}Te impossible. As a result of the weak dependence on higher lying levels only the first four states of ^{130}Te were used in the calculations.

The situation is considerably different for the case of ^{122}Te. For example, with the matrix elements of fig. 5 a change in the sign of the interference term changes Q_{2+} by about 0.2 $e \cdot b$. Moreover in order to determine Q_{2+} with an accuracy of $\pm 0.05\ e \cdot b$ the absolute values of the matrix elements M_{23} and M_{24} must be known with a precision of better than ± 20 %. Values for the matrix elements of the 2_2^+ and 4_1^+ levels were obtained from the excitation probabilities for these levels [14]) and from the branching [15]) and mixing ratios [16]). The values found in ref. [14]) were in reasonable agreement with those of Barrette *et al.* [5]).

Contributions to the excitation probabilities via levels above the 0_2^+ state of ^{122}Te at 1.357 MeV were also considered. Using the values of 0.069 $e \cdot b$ for M_{16} and 0.26 $e \cdot b$ for M_{26} from ref. [5]) we find that the influence (i.e. a change in sign of M_{16}) of a 2_3^+ level at 1.752 MeV is to induce a change in the Q_{2+} of about 0.03 $e \cdot b$. The 3^- state at 2.17 MeV can contribute to R_{2+} via interference terms of the form $\langle 0_1^+||E3||3^-\rangle\langle 3^-||E1||2_1^+\rangle\langle 0_1^+||E2||2_1^+\rangle$ or $\langle 0_1^+||E3||3^-\rangle\langle 3^-||E3||2_1^+\rangle\langle 0_1^+||E2||2_1^+\rangle$. Both terms have been investigated by taking $\langle 0_1^+||E3||3^-\rangle = 0.16\ e^2 \cdot b^3$ [ref. [14])]. The $\langle 3^-||E1||2_1^+\rangle$ value was varied from 10^{-4} to 10^{-1} W.u., which changed R_{2+} by less than 0.02 %. The second term, taking $\langle 3^-||E3||2_1^+\rangle = \langle 0_1^+||E3||3^-\rangle$, was found to contribute less than 0.4 % to R. Hence both terms have been neglected in the analysis. Due to the uncertainty in the relevant matrix elements the influence [17]) of the giant dipole resonance and hexadecapole moments have similarly been neglected.

The excitation probabilities have been corrected for effects due to vacuum polar-

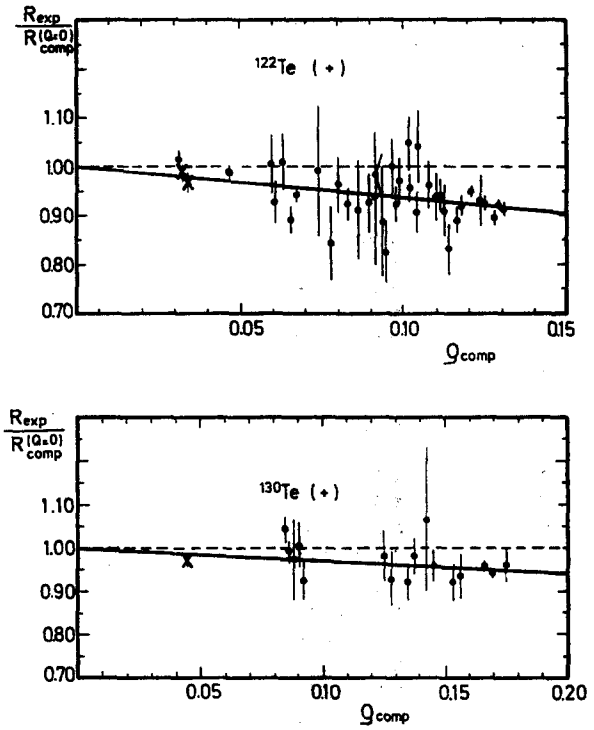

Fig. 6. The ρ-plots and fits to the data for the positive interference sign. The ^{16}O data are denoted by solid circles, the ^{4}He data by a cross.

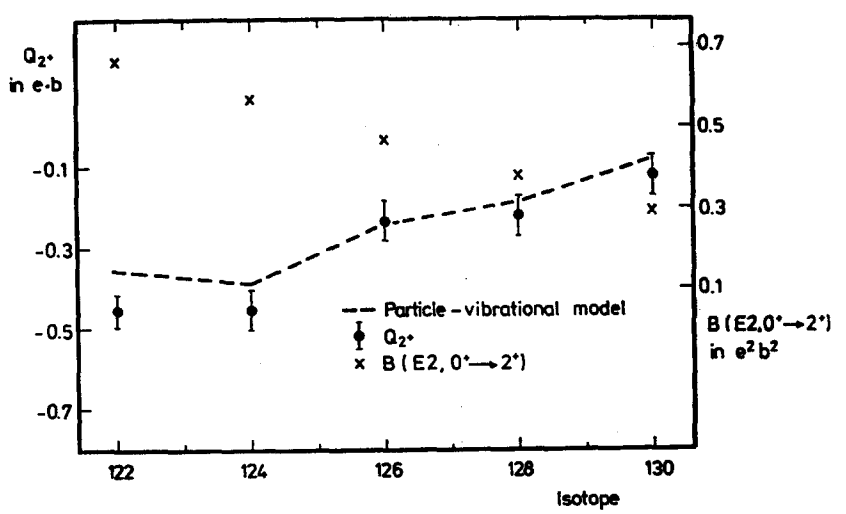

Fig. 7. Weighted averages of the Q_{2+} and $B(E2, 0^+ \rightarrow 2^+)$ values of the even tellurium isotopes taken from refs. [2-7]) and the present work. Also shown are the results of the particle vibrational coupling model from ref. [26]).

TABLE 3

The experimental results and weighted averages obtained in the present work and refs. [2-7])

Isotope	$Q_{2^+}(e \cdot b)$	$B(E2, 0^+ \rightarrow 2^+)$ $(e^2 \cdot b^2)$	Sign of interf. term	Ref.
122	−0.21±0.08		−	[4])
	−0.43±0.08		+	[4])
	−0.20±0.10	0.665±0.011	−	[5])
	−0.46±0.10	0.667±0.011	+	[5])
	−0.22±0.05	0.658±0.004	−	pres. work
	−0.48±0.05	0.658±0.004	+	pres. work
	−0.21±0.04	0.659±0.004	−	av.
	−0.47±0.04	0.659±0.004	+	av.
124	−0.28±0.08		−	[4])
	−0.49±0.08		+	[4])
	−0.11±0.10	0.568±0.011	−	[5])
	−0.46±0.10	0.571±0.011	+	[5])
	−0.16±0.08	0.566±0.005	−	[6])
	−0.41±0.08	0.568±0.005	+	[6])
	−0.19±0.05	0.566±0.005	−	av.
	−0.45±0.05	0.569±0.005	+	av.
126	−0.16±0.11	0.486±0.035	−	[2])
	−0.32±0.11	0.487±0.035	+	[2])
	−0.20±0.10	0.478±0.011	−	[5])
	−0.28±0.10	0.479±0.011	+	[5])
	+0.02±0.11	0.466±0.007	−	[6])
	−0.14±0.11	0.467±0.007	+	[6])
	−0.10±0.09		−	[7])
	−0.20±0.09		+	[7])
	−0.11±0.05	0.470±0.006	−	av.
	−0.23±0.05	0.471±0.006	+	av.
128	−0.11±0.10	0.389±0.029	−	[2])
	−0.21±0.13	0.391±0.029	+	[2])
	−0.26±0.11	0.387±0.011	−	[5])
	−0.33±0.11	0.387±0.011	+	[5])
	+0.08±0.09	0.377±0.006	−	[6])
	−0.12±0.09	0.378±0.006	+	[6])
	−0.14±0.08		−	[7])
	−0.24±0.08		+	[7])
	−0.10±0.05	0.380±0.005	−	av.
	−0.22±0.05	0.380±0.005	+	av.
130	−0.12±0.15	0.30 ±0.03	−	[3])
	−0.19±0.15	0.30 ±0.03	+	[3])
	+0.00±0.08		−	[4])
	−0.08±0.08		+	[4])
	−0.09±0.12	0.290±0.011	−	[5])
	−0.14±0.12	0.290±0.011	+	[5])
	−0.07±0.10	0.295±0.006	−	pres. work
	−0.15±0.10	0.296±0.006	+	pres. work
	−0.05±0.05	0.294±0.005	−	av.
	−0.12±0.05	0.294±0.005	+	av.

The asterisks indicate values corrected due to the deorientation effect [6]). In the present work χ^2 was 1.1 for ^{122}Te and 0.7 for ^{130}Te, independent of the sign of the interference term.

ization and screening due to atomic electrons [18]). It is found that these effects are largely energy and projectile mass independent. Their sum is found to produce a change in R of between $-0.2\,\%$ at 44° and $+0.3\,\%$ at 173°. Quantal corrections [19]) were also made and result in an increase in the $B(\mathrm{E2}, 0_1^+ \rightarrow 2_1^+)$ by about 0.003 $e^2 \cdot \mathrm{b}^2$, and have a negligible effect on the Q_{2+}.

Results of the analysis are shown in fig. 6, where the ratio $R_{\mathrm{exp}}/R_{\mathrm{comp}}(Q_{2+} = 0)$ has been plotted against the sensitivity parameter ρ_{comp} as described in ref. [8]). Values for Q_{2+} and the $B(\mathrm{E2}, 0_1^+ \rightarrow 2_1^+)$ were obtained for both the positive and the negative signs of the interference term and are listed in table 3. For ^{122}Te only the results for which the sign of the interference term involving the 2_3^+ state was the same as that for the 2_2^+ state are given.

Although the separate analysis of the projectile mass and scattering angle dependence can in principle distinguish between these signs, the statistical accuracy of the data combined with the small magnitude of the interference term yields too small an effect to obtain the sign with any degree of confidence. However, recent measurements [refs. [20-22])] of the interference term sign for nuclei in this region as well as model predictions [23-25]) for these nuclei all indicate a positive sign for this term. We have therefore adopted this sign in the discussion which follows.

4. Discussion

In table 3 the results of the present work and those of refs. [3-5]) together with the adopted average values for Q_{2+} and the $B(\mathrm{E2}, 0_1^+ \rightarrow 2_1^+)$ values are shown. As is seen the agreement among the various measurements is excellent for both the Q_{2+} and the $B(\mathrm{E2}, 0_1^+ \rightarrow 2_1^+)$ values. This agreement is exhibited for the measurements of all Te isotopes as shown in table 3 and is particularly gratifying in light of the difficulties previously encountered in reorientation effect measurements [1]). Indeed, the agreement and high statistical accuracy of the results allows a set of very precise Q_{2+} (about $\pm 0.05\, e \cdot \mathrm{b}$) and $B(\mathrm{E2}, 0_1^+ \rightarrow 2_1^+)$ values to be adopted from the averages of the measurements listed in table 3.

The average values of the Q_{2+} and $B(\mathrm{E2}, 0_1^+ \rightarrow 2_1^+)$ from table 3 are plotted in fig. 7 as a function of isotope number. This figure reinforces the tendency previously [6]) noted in which the $|Q_{2+}|$ decreases with increasing neutron number. The improved accuracy enables one to discern some structure in this dependence. In particular, the jump of Q_{2+} from -0.45 at 124 to -0.23 at 126 might possibly be associated with some underlying single particle structure. Also shown are the predictions of the particle vibrational coupling model [26]) which should reflect the single particle behaviour of the valence neutrons and does indeed seem to reproduce the neutron number dependence of Q_{2+}.

References

1) Proc. Topical Conf. on problems of vibrational nuclei, Zagreb, 1974, ed. G. Alaga, V. Paar and L. Sips (North-Holland, Amsterdam, 1975)
2) R. G. Stockstad and I. Hall, Nucl. Phys. **A99** (1967) 507
3) A. Christy, I. Hall, R. P. Harper, I. M. Naqib and B. Wakefield, Nucl. Phys. **A142** (1970) 591
4) R. D. Larsen, W. R. Lutz, T. V. Ragland and R. P. Scharenberg, Nucl. Phys. **A221** (1974) 21
5) J. Barette, M. Barette, R. Harutunian, G. Lamoureux and S. Monaro, Phys. Rev. **C10** (1974) 1166
6) A. M. Kleinfeld, G. Mäggi and D. Werdecker, Nucl. Phys. **A248** (1975) 342
7) T. V. Ragland, R. J. Mitchell and R. P. Scharenberg, Nucl. Phys. **A250** (1975) 333
8) J. de Boer and J. Eichler, in Advances in nuclear physics ed. M. Baranger and E. Vogt, vol. 1 (Plenum Press, New York, 1968) p. 1
9) Z. Berant, R. A. Eisenstein, Y. Horowitz, U. Smilanski, P. N. Tandon, T. S. Greenberg, A. M. Kleinfeld and H. G. Mäggi, Nucl. Phys. **A196** (1972) 312
10) A. Bockisch, J. Dickers, W. Klein and A. M. Kleinfeld, to be published
11) P. H. Stelson and L. Grodzins, Nucl. Data **A1** (Academic Press, New York, 1965) p. 21
12) B. C. Robertson and J. T. Sample, Phys. Rev. **C4** (1971) 2176
13) A. Winther and J. de Boer, California Institute of Technology, Technical Report, November 18, 1965
14) A. Bockisch, M. Miller and A. M. Kleinfeld, to be published
15) K. S. Krane, Phys. Rev. **C10** (1974) 1197
16) J. Koch, W. Münnich and V. Schötzig, Nucl. Phys. **A103** (1967) 300
17) O. Häuser, D. Pelte, T. K. Alexander and H. C. Evans, Nucl. Phys. **A150** (1970) 417
18) M. Miller, Diplomarbeit, Köln (1975)
19) K. Alder, F. Rosel and R. Morf, Nucl. Phys. **A186** (1972) 449
20) R. D. Larsen, J. A. Thomson, R. G. Kerr, R. P. Scharenberg and W. R. Lutz, Nucl. Phys. **A195** (1972) 119
21) L. Hasselgren, C. Fahlander, L. O. Edvardson, J. E. Thun, F. Falk and B. S. Ghumman, UUIP-897
22) C. Fahlander, L. Hasselgren, J. E. Thun, A. Bockisch, A. M. Kleinfeld, A. Gelberg and K. P. Lieb, to be published
23) T. Tamura. Phys, Lett. **28B** (1968) 90
24) V. I. Isakov and I. Kh. Lemberg, JETP Lett. (Sov. Phys.) **9** (1969) 438
25) K. Kumar, Phys. Lett. **29B** (1969) 25
26) E. Degrieck and G. Vanden Berghe, Nucl. Phys. **A231** (1974) 141